



Stockholm
University

Bachelor Thesis

Degree Project in
Geology 15 hp

Mineralogy and petrology of a drill core section from Borg, SW Norrköping – fracture fillings and tentative mineral reactions

Ting-Fung Chong



Stockholm 2019

Department of Geological Sciences
Stockholm University
SE-106 91 Stockholm

Preface

This bachelor thesis is done for the Institution of Geoscience at Stockholm University. The thesis corresponds to 15 points of a bachelor's degree in geoscience. The thesis is done in cooperation with Trafikverket (The Swedish Transport Administration) in connection with the railroad project Ostlänken southwest of Norrköping.

Main supervisor of this project is Joakim Mansfeld, Stockholms University. Karl-Johan Lorents, Trafikverket is co-supervisor. Assistance of XRD analyses are Andreas Karlsson, Naturhistoriska Riksmuseet and Jenny Sjöström, Stockholms University.

Thanks to Karl-Johan Lorents for this project and Joakim Mansfeld, Andreas Karlsson and Jenny Sjöström for assistance.

Stockholm, June 2019

Ting-Fung Chong

Table of contents

Abstract	3
1. Introduction	4
1.1 Regional geology	4
1.2 Local geology.....	5
1.3 Legend from SGU, map series K439.....	6
1.4 Description of the drill core	7
1.5 Secondary reactions and replacement	7
1.6 Mineralogy of phyllosilicates	11
2. Methods.....	14
2.1 Microscope.....	14
2.2 Thin sections	14
2.3 XRD (X-ray Powder Diffraction).....	15
2.4 XRF (X-ray Fluorescence).....	15
3. Result	16
3.1 Microscope.....	16
3.2 Thin section.....	17
3.3 XRD.....	22
3.4 XRF	24
4. Discussion.....	25
4.1 Fine-grained mafic rock	25
4.2 Contact	27
5. Conclusions	27
6. Further studies	28
7. References	29

Abstract

During drilling at Borg, ca. 5 km southwest of central Norrköping, an unidentified fine-grained grey rock was encountered in contact with dark red granitic gneiss at 35m depth. The fine-grained grey rock occurs above the red granitic gneiss. Our understanding prior to testing is that the rock may have been formed by fluid alteration of a mafic rock, as neither metamorphic nor sedimentary textures were observed. Understanding this rock and the formation processes related to it, is of interest for the general understanding of the region and of geotechnical importance since fracture fillings may affect the stability of the rock during and after construction projects. This study uses the methods petrography, XRD and XRF to define the fine-grained mafic rock, black vein in the fine-grained mafic rock, the contact zone and the granitic gneiss. Results show that the fine-grained grey rock has a composition of muscovite (36.1%), quartz (24.6%), albite (20.8%), sericite (10.8) and montmorillonite (0.5%). The contact is mainly made of quartz veins and calcite veins. The protolith of the fine-grained mafic rock is suggested to be iron-rich. Further testing on additional unaltered mafic rock samples from the area would provide a more accurate picture of the protolith evolution.

1. Introduction

At Borg, 5 km southwest of central Norrköping, a drill core extracted by Trafikverket was found to contain a grey rock of unknown identity. The drill core also contained a dark red granitic gneiss, a thin white contact zone between these two rocks, as well as thin black veins in the unidentified grey rock. SGU suggest a mafic origin of the grey rock. This project aims at characterising the fine-grained mafic rock and its origin, as well as finding a plausible explanation for its formation. This is important as calculations for the construction project are based on the physical properties of the rock. Chemical properties are important as some minerals may dissolve in presence of water resulting in weakening of rock and/or leakage.

1.1 Regional geology

The region belongs to the Svecofennian orogen, which is associated with multiple phases of magmatism, tectonic events and regional metamorphism of the Baltic Shield/ Fennoscandian Shield during 2.0 – 1.8 Ga. The culmination of orogenesis occurred at 1.9 – 1.8 Ga. This orogeny covers the eastern to north-eastern part of Sweden and south-western part of Finland. The area of Sweden is divided into three regions: northern, middle and southern, and are defined by different tectonic events (Lundqvist, 2011).

The location of study is in the central part of the southern region know as Bergslagen, the southern region is dominated by Paleoproterozoic rocks formed during and affected by orogeny. The western part of the region was later overprinted by a Sveconorwegian tectonic event between 1.0 – 0.9 Ga (Stephens, 2009). There are volcanic, plutonic and sedimentary rocks in this region which have varied grade of metamorphism in different locations. The volcanic rocks in this region are dominated by felsic types from rhyolitic to dacitic but intermediate to mafic types can also be found. Granitoids are the most common plutonic rock in this region. Granitoid intrusions are common, as well as mafic to ultramafic intrusions and mixed intrusions containing both felsic and mafic mineral due to mingling can also be found (Lundqvist, 2011). The granitoid intrusions occur during two periods; 1.5 Ga and 1.47 Ga in the north-eastern respective north-western part of Bergslagen. Meanwhile the mafic to ultramafic intrusions occur as four sequences: 1.6 – 1.56 Ga (south), 1.48 – 1.46 Ga (north-western and north-east), 1.27 – 1.26 Ga (north-east) and 0.98 – 0.95 Ga (west), Stephens, 2009. The sedimentary rocks from this period are either volcanic or deposited during rifting (Lundqvist, 2011).

1.2 Local geology

This area (**fig 1**) is dominated by granite or granitic gneiss. Some outcrops of quartz-feldspar-rich Svecofennian high-grade metasedimentary rocks that also can be found 5 km southwest and directly to the north (1.25 km). Furthermore, mafic to ultramafic intrusions in the region most likely formed during the 1.6 – 1.56 Ga event. There are different intrusion compositions of different ages (see **section 1.3** for legend) spread across this area with some small felsic metavolcanic outcrops.

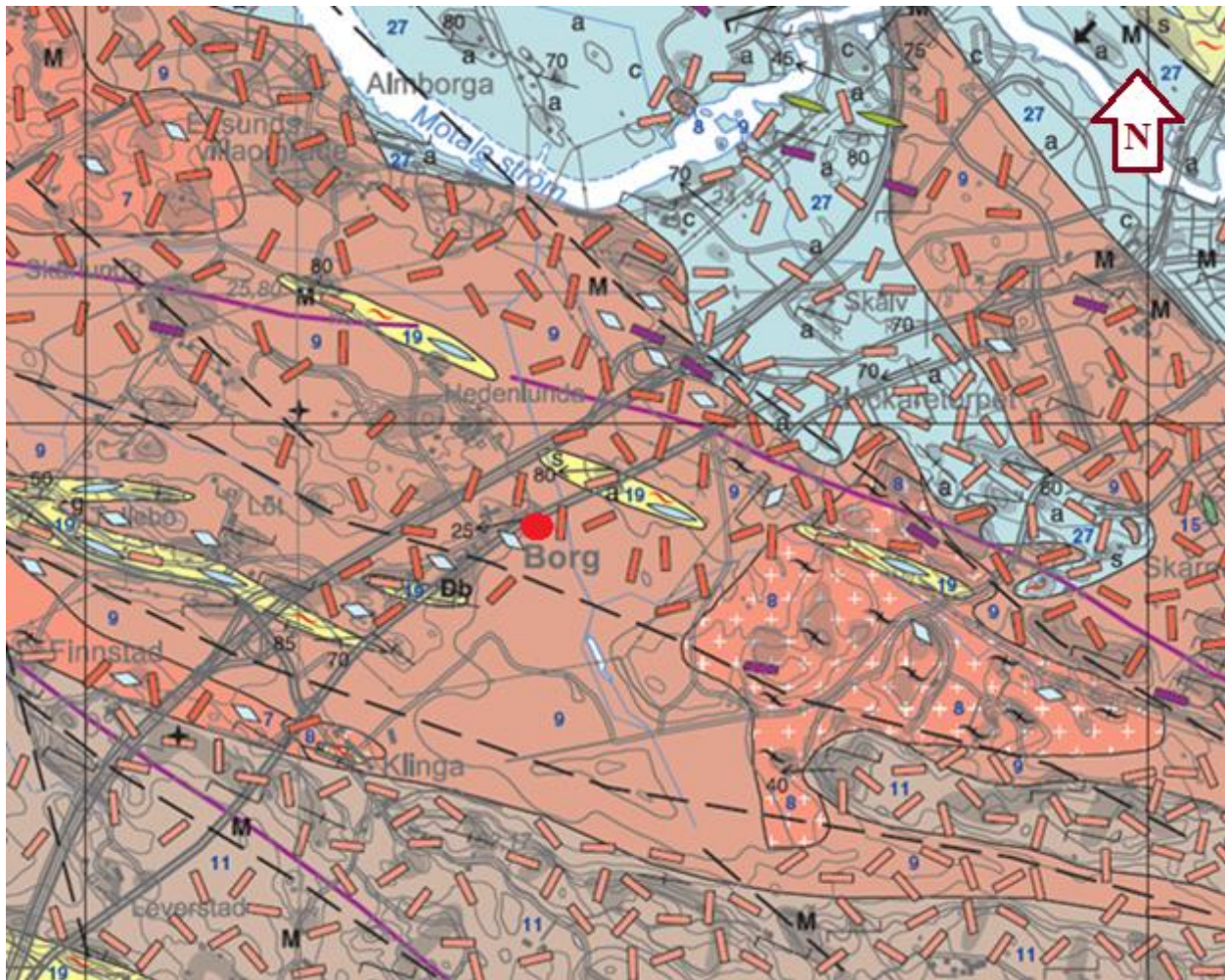
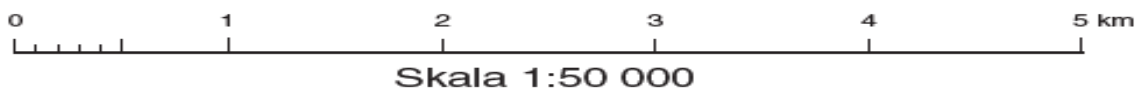








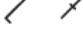

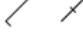

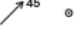



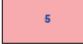

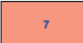

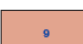
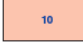








Figure 1: Map of locality, red circle shows approximate location of drill hole. SGU map series K 439, 2013.



1.3 Legend

Legend from SGU, map series K439

<p> Ådrad (metatexit), t.v., kraftigt uppsmält (diatexit), t.h. <i>Metatexitic, left, diatexitic, right</i></p> <p> Glimmerstrimmighet <i>Mica schlieren</i></p> <p>a g Andalusit (a), cordierit (c), granat (g), hornblände (h) c h <i>Andalusite (a), cordierite (c), garnet (g), hornblende (h)</i></p> <p>m t Muskovit (m), sillimanit (s), turmalin (t) s <i>Muscovite (m), sillimanite (s), tourmaline (t)</i></p> <p>Db S Diabas (Db), pegmatit (P), skarn (S) P <i>Dolerite (Db), pegmatite (P), skarn (S)</i></p> <p> Xenolit, kantig; metamafit, t.v., metamorf bergart, ospecificerad, t.h. <i>Xenolith, angular; metamafic rock, left, metamorphic rock, unspecified, right</i></p> <p> Xenolit, delvis assimilerad, kantig, metamorf bergart, ospecificerad <i>Xenolith, partly assimilated, angular, metamorphic rock, unspecified</i></p> <p> Gång, <50 m bred; pegmatit, t.v., metabasit, t.h. <i>Dyke, <50 m wide; pegmatite, left, metabasic rock, right</i></p> <p> Metabasit, inlagring <i>Metabasic rock, lens</i></p> <p>M B Mylonit, t.v., förkastningsbreccia, t.h. <i>Mylonite, left, breccia, right</i></p> <p> Stenbrott, krossberg, täkt i drift <i>Quarry, aggregates, in operation</i></p> <p> Deformationszon, ospecificerad <i>Deformation zone, unspecified</i></p> <p> Lagring; okänd stupning, t.v., vertikal stupning, t.h. <i>Bedding; dip direction and dip unknown, left, dip vertical, right</i></p> <p> Foliation, gradtal för stupning <i>Foliation, dip in degrees</i></p> <p> Foliation; okänd stupning, t.v., vertikal stupning, t.h. <i>Foliation; dip direction and dip unknown, left, dip vertical, right</i></p> <p> Foliation med vindlande strykning; vertikal, t.v., känd stupningsriktning, okänt antal grader, t.h. <i>Foliation with undulating strike direction; vertical, left, dip direction indicated, dip unknown, right</i></p> <p> Stänglighet; gradtal för stupning, t.v., vertikal, t.h. <i>Lineation; plunge in degrees, left, vertical, right</i></p>	<p>Mesoproterozoiska intrusiva bergarter (ca 1,55 miljarder år) <i>Mesoproterozoic intrusive rocks (c. 1.55 Ga)</i></p> <p> Diabas <i>Dolerite</i></p> <p>Paleoproterozoiska, postsvekokarelska intrusivbergarter (ca 1,81–1,75 miljarder år) <i>Palaeoproterozoic, post-Sveco Karelian intrusive rocks (c. 1.81–1.75 Ga)</i></p> <p> Granit, aplit, <50 m bred gång <i>Granite, aplite, <50 m wide dyke</i></p> <p>Paleoproterozoiska, postsvekokarelska intrusivbergarter (ca 1,85–1,65 miljarder år) <i>Palaeoproterozoic, post-Sveco Karelian intrusive rocks (c. 1.85–1.65 Ga)</i></p> <p> Granit, kvartsmonzonit, <50 m bred gång <i>Granite, quartz monzonite, <50 m wide dyke</i></p> <p> Granit, medelkornig, ojämnkornig, radiumindex 0,2±0,02, aktivitetsindex 1,2±0,1 <i>Granite, medium-grained, uneven-grained</i></p> <p>Paleoproterozoiska yt- och intrusivbergarter mer eller mindre påverkade av svekokarelsk deformation och metamorfos (ca 1,85–1,75 miljarder år) <i>Palaeoproterozoic supracrustal and intrusive rocks affected, to a variable extent, by Sveco Karelian deformation and metamorphism (c. 1.85–1.75 Ga)</i></p> <p>Senorogena intrusivbergarter (ca 1,85–1,75 miljarder år) <i>Late-orogenic rocks (c. 1.85–1.75 Ga)</i></p> <p> Granit, <50 m bred gång <i>Granite, <50 m wide dyke</i></p> <p> Granit till granodiorit, röd, radiumindex 0,3, aktivitetsindex 1,1 <i>Granite to granodiorite, red</i></p> <p> Pegmatit med aplitgranit och aplit, radiumindex 0,03, aktivitetsindex 0,4 <i>Pegmatite with aplitic granite and apite</i></p> <p> Granodiorit till granit, grå, radiumindex 0,3±0,2, aktivitetsindex 0,9±0,3 <i>Granodiorite to granite, grey</i></p> <p>Tidigorogena intrusivbergarter (ca 1,95–1,85 miljarder år) <i>Early-orogenic intrusive rocks (c. 1.95–1.85 Ga)</i></p> <p> Granit, gnejsig, radiumindex 0,2±0,02, aktivitetsindex 0,6±0,2 <i>Granite, gneissic</i></p> <p> Granodiorit, gnejsig, radiumindex 0,2±0,1, aktivitetsindex 0,7±0,1 <i>Granodiorite, gneissic</i></p> <p> Tonalit, gnejsig, radiumindex 0,1, aktivitetsindex 0,6 <i>Tonalite, gneissic</i></p> <p>Svekofenniska ytbergarter (ca 2,0–1,87 miljarder år) <i>Svecofennian supracrustal rocks (c. 2.0–1.87 Ga)</i></p> <p> Felsisk metavulkanisk bergart, skiktad (tufftisk), inlagringar av metasedimentära bergarter, radiumindex 0,2±0,04, aktivitetsindex 0,7±0,2 <i>Felsic metavolcanic rock, tuffitic, lenses of metasedimentary rocks</i></p> <p> Metagråvacka, metaargillit, inlagring <i>Metagreywacke, metaargillite, lens</i></p> <p> Xenolit, kantig, metasedimentär bergart <i>Xenolith, angular, metasedimentary rock</i></p> <p> Glimmerskiffer med metaarenit, andalusitförande, radiumindex 0,2±0,02, aktivitetsindex 0,8±0,1 <i>Mica schist with metaarenite, andalusite-bearing</i></p>
---	--

1.4 Description of the drill core

The fine-grained mafic rock is microcrystalline and lacks foliation. Multiple black veins can also be observed in the fine-grained mafic rock. The rock is reddish brown at the contact. See **fig 2** for overview of the drill core sample.

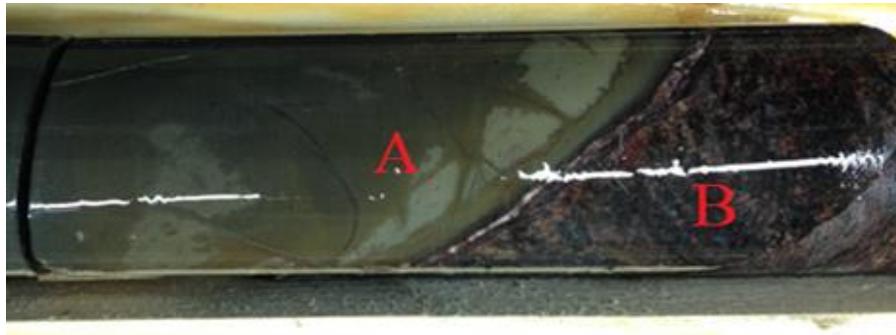
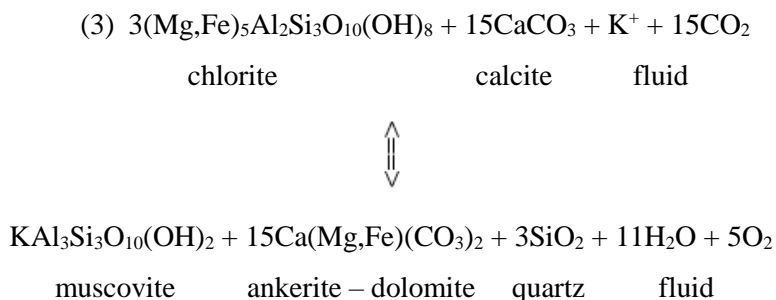


Figure 2: shows the drill core sample where the fine-grained grey rock (A) and dark red granitic gneiss (B) can be observed with the white contact between these two rock types. The length of this piece is 10cm.

1.5 Secondary reactions and replacement

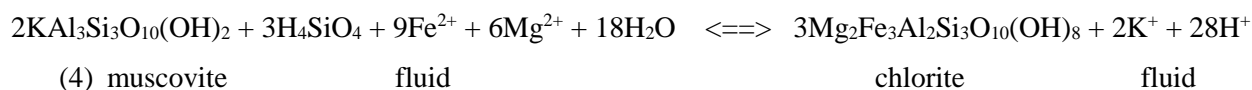
Clay minerals are produced by weathering (sedimentary process) or alteration of rock. Different rock and alteration processes result in different products which can assist understanding the original rock before alteration. Rocks may be altered in an open system after formation, which results in chemical and mineralogical changes. The changes are categorised into metamorphism, metasomatism, hydrothermal and deuteritic alteration (Mathieu, 2018). Metamorphism starts between 100 - 150°C (Winter, 2014, p51). Deuteritic alteration is a process of late stage magmatic fluids which occurs below metamorphism temperature. Compared to metamorphism, deuteritic alteration preserves the pre-existing texture while metamorphism changes it to a foliated texture. The definitions of metasomatism and hydrothermal alteration have secondary fluids as their fluid source. It can be difficult to distinguish processes like diagenesis (sediments become rock) and low-grade metamorphism below 150°C. Insights of original rock can be gained by observing the alteration products and characteristics of the system as temperature of stability can be seen in **fig 3**. This may help with identification of the original mineral composition. This section summaries the basic concepts of fluid alteration processes explained using mass balance calculations (Mathieu, 2018). An overview of alteration processes, their associated chemical changes and alteration minerals can be observed in **Table 1**.

The carbonates may destabilise chlorite to produce muscovite, anhydrous carbonates (ankerite – dolomite) and quartz according to



Chloritisation

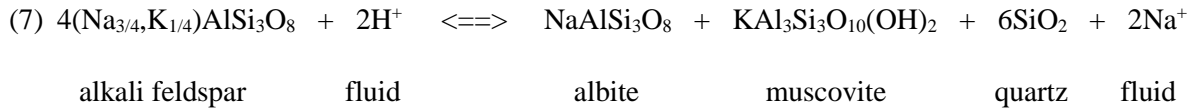
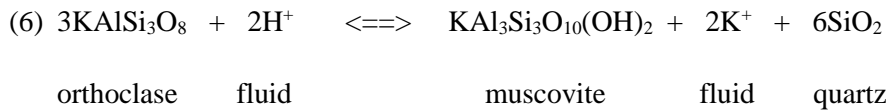
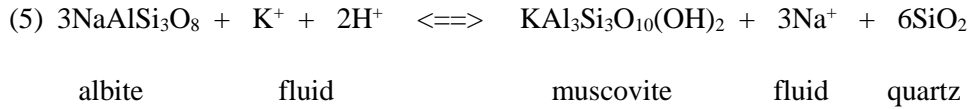
Chloritisation is a form of alteration that affects any mafic mineral and replace it with the mineral chlorite $\text{X}(\text{Mg, Fe}^{2+}, \text{Fe}^{3+}, \text{Mn, Ni, Na, Li, Al, Ti})_{4-6}\text{Y}(\text{Si, Al})_4\text{O}_{10}(\text{OH})_8$. Chlorite is a very hydrous phyllosilicate and replaces less hydrous mafic minerals at low temperature when water becomes available. Pyroxenes and amphiboles are commonly affected by various stages of chloritisation (Winter, 2014), the chloritisation of olivine is difficult to prove whether it is superficial or a deep-seated process (Mathieu, 2018). The replacement is like any other hydrothermal alteration occurs at the rim and works inward. In presence prominent cleavages like biotite, the alteration may also affect the cleavage at the same time (Winter, 2014, p51). Chloritisation corresponds to gains of variable X elements. Increase of X induces mineralogical changes as these elements combine with Si (could also be transported by fluid) and the less mobile Al to form chlorite. An example of this process is chloritisation of muscovite which also induces K-loss and increased acidity of the fluid (see equation 4). Chloritized rocks display gains of Fe and/or Mg and loss of Ca, Na, and/or K depending on the type of feldspar (Mathieu, 2018).



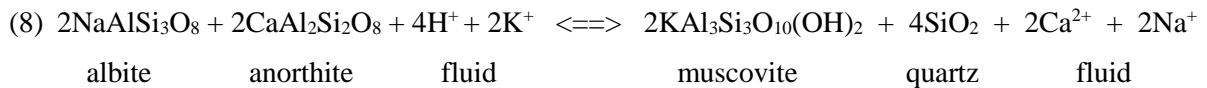
Sericitisation

Sericitisation is an acidic alteration that produces muscovite with sericitic texture. This alteration process requires K^+ either in the alteration mineral or in fluid. In case of feldspar, alkali feldspar will induce loss of K^+ if it contains more than 1K^+ per alkali feldspar reaction (equation 5-8). While

plagioclase feldspar requires K^+ in the fluid and induces gain of K^+ . Sericitisation results in Ca- and Na-losses with K-gain or loss depending on the type of feldspar being altered (Mathieu, 2018). The following equations shows albite (5), orthoclase (6), alkali feldspar (7) and plagioclase feldspar (8) sericitisations: (Mathieu, 2018)



Na can also be present in the fluid instead as part of the alkali feldspar.



Albitisation and K-feldspar alterations

These processes correspond to the composition of feldspar and changing concentration of Na and K. Feldspar with high concentration of Na limits the production of muscovite and quartz as it has less amount of reacting K unless the fluid has high K concentration. High K concentration feldspar increases the production of muscovite and quartz while increasing the K concentration in fluid as well (equation 5-8)(Mathieu, 2018).

Sulphidation

Sulphidation correlates the concentration of S in fluids with metals such as Fe in the fluid or host rock to form FeS_2 and/or other sulphides.

Table 1.: Alteration processes, associated chemical changes and alteration minerals (Mathieu, 2018).

	Mass Changes	Examples of Assemblages
Sulphidation	+S, +metals	Any minerals + sulphides
Silicification	+Si	Any minerals + quartz
Carbonatisation	+C, +Ca	Carbonates ± quartz, mica, chlorite
Sericitisation	+K or -K, -Na, -Ca, +H	Mica + quartz
Chloritisation	+Fe, +Mg, +X, +H, -Na, -Ca, -K	Chlorite + mica ± quartz, pyrite
K-feldspar alteration	+K, - Na	K-feldspar + mica + quartz
Albitisation	+Na, -K	Albite + hornblende ± biotite, quartz

1.6 Mineralogy of phyllosilicates

Phyllosilicates can be produced by different processes and by identifying the type in the sample it could provide and support the acknowledge of the origin. Clay refers to a mineral group of hydrous aluminosilicates with a predominating size $<2 \mu\text{m}$. They resemble, in chemical and structural composition, the minerals of rocks originating from the crust of the earth. When rocks experience changes from elevated temperatures and high pressure to a less pressurised and/or cooler and/or more hydrous surrounding such as ascending toward surface of the earth, the rocks become unstable and are easily affected by alteration or weathering, which results in hydrous minerals. The alteration process is due to incongruent reactions while the precipitation or recrystallisation of dissolved contents into more stable forms is due to congruent reaction (Lal, 2002). **Fig 4** Shows example of different common minerals and their resistance compared to each other.

Pyrite Dolomite Ca-plagioclase Ca/Na-plagioclase Biotite Muscovite Quartz Gibbsite
 Calcite Olivine Pyroxene Amphiboles K-feldspar Smectite Kaolinite Hematite

Figure 4: Shows increasing resistance to alteration from left toward right. Primary minerals are generally less resistant to alteration than secondary minerals. Grain size also affects the speed of alteration and weathering (Carroll, 1970).

These silicates contain continuous two-dimensional tetrahedral sheets with composition T_2O_5 where T is tetrahedral cation such as Si, Al or Fe^{3+} . Each individual tetrahedra is linked with nearby tetrahedra by sharing three corners each (the basal oxygens) to form a hexagonal mesh pattern. The fourth tetrahedra corner (the apical oxygen) points in a direction normal to the sheet and is a part of the direct adjacent octahedral sheet which consist of individual octahedra laterally sharing octahedral edges. Except sharing the apical oxygen between the layers there is also a unshared OH group which may be replaced by F. The common octahedral cations are Mg, Al, Fe^{2+} and Fe^{3+} , the octahedral cation may be replaced by other medium-sized cations such as Li, Ti, V, Cr, Mn, Co, Ni, Cu and Zn. There are two assemblage of tetrahedral and octahedral sheets (**fig 5.**). The first assemblage is called 1:1 layer which is one tetrahedral sheet linked with one octahedral sheet, in such layer the unshared plane of anions in the octahedral sheet is only consisted by OH groups. The second assemblage is called 2:1 layer which is two tetrahedral sheets linked together with an octahedral sheet between them. If the 1:1 or 2:1 is not electrostatic neutral then it is neutralised by interlayering material such as individual cations, hydrated cations and hydroxide octahedral groups and/or sheets. A structure unit is the measurement of the total assemblage of a layer plus interlayer (Brindley, 1984).

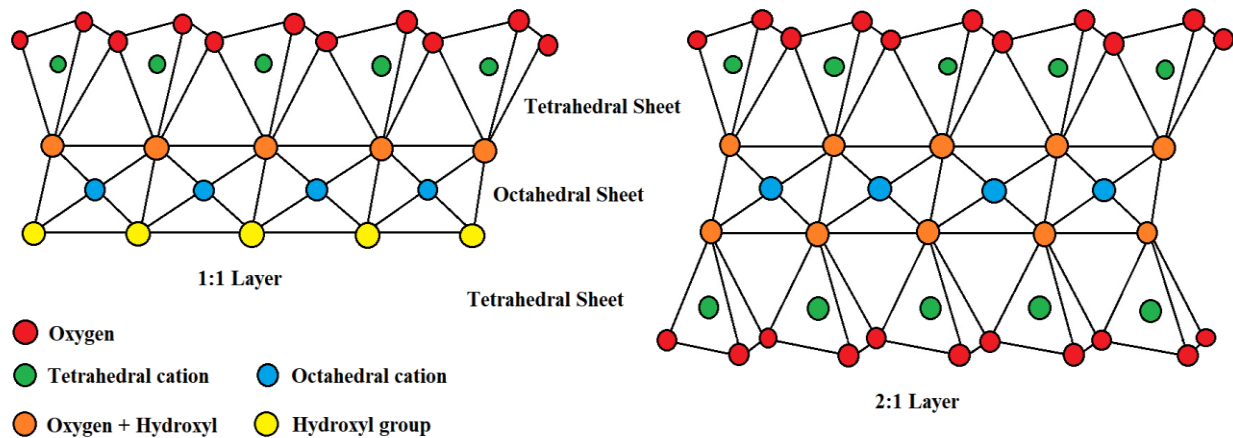


Figure 5: Three-dimensional view of 1:1 and 2:1 layer (Brindley, 1984; modified by Chong, 2019).

Clay minerals can be classified by layer type (1:1 or 2:1), layer charge (x) and interlayer type into eight major groups; serpentine, kaolin, talc, pyrophyllite, smectite, vermiculite, mica, brittle mica, chlorite and sepiolite-palygorskite. Further division into sub-groups (**Table 2**) are related to octahedral sheet type (dioctahedral or trioctahedral), chemical composition, geometry of individual layers and interlayers. These groups and subgroups result in different lateral dimensions that can be used to distinguish them from each other by using XRD which measures in Å ($1\text{Å} = 0.1$ nanometer); see **Fig 6.** (Brindley, 1984).

Figure 6: Structures of major clay mineral groups view from direction [010], layer charge per formula unit (x) and lateral dimension in Å

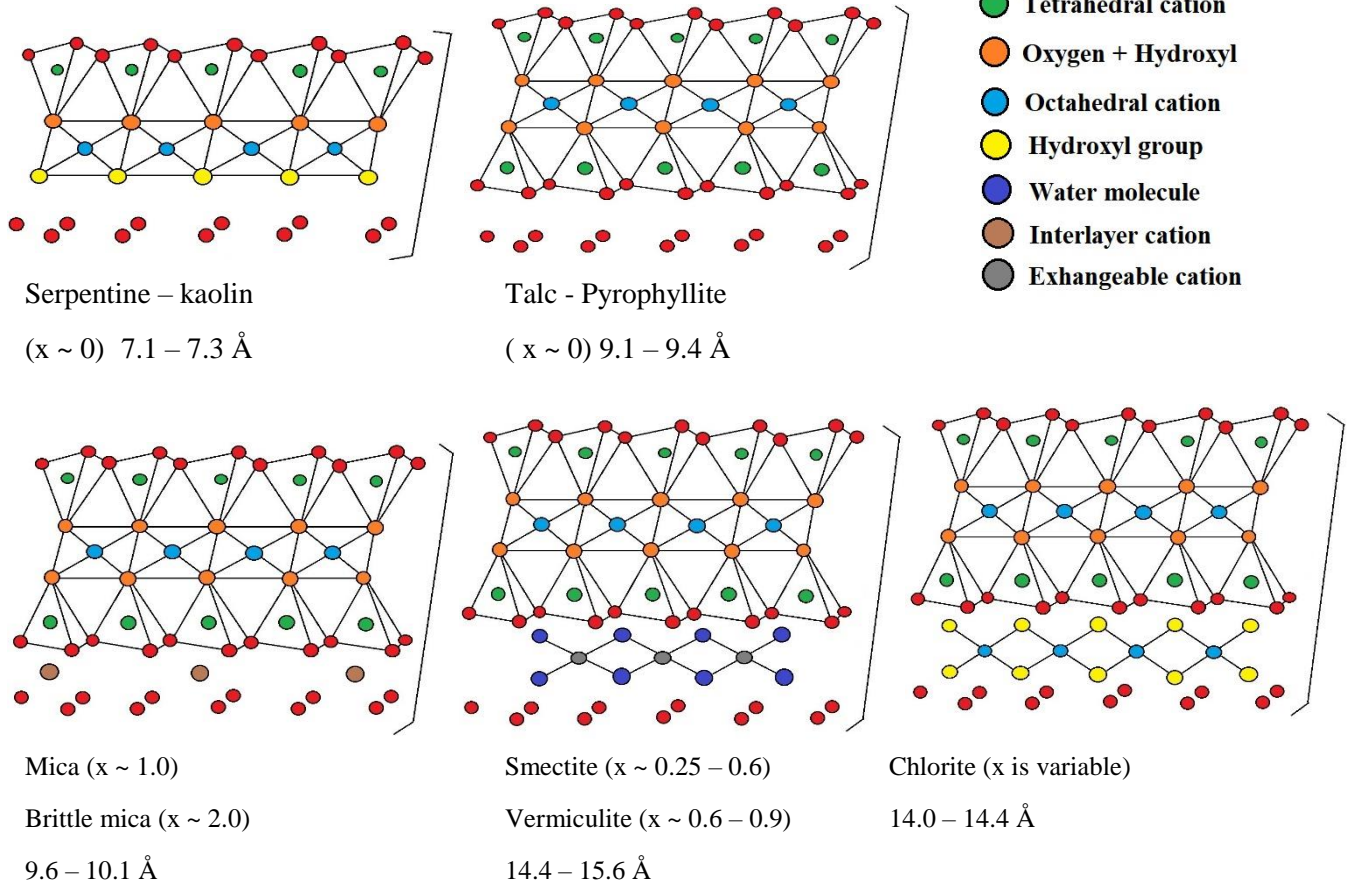


Table 2: Classification of clay minerals of group, sub-group and example of species (Brindley, 1984).

Layer type	Group	Sub-group	Example of species
1:1	Serpentine - kaolin	Serpentines	Chrysotile, antigorite, lizardite, amesite
		Kaolins	Kaolinite, dickite, nacrite
2:1	Talc - pyrophyllite	Talcs	Talc, willmenseite
		Pyrophyllite	Pyrophyllite
	Smectite	Saponites	Saponite, hectorite, sauconite
		Montmorillonites	Montmorillonite, beidellite, nontronite
	Vermiculite	Trioctahedral vermiculites	Trioctahedral vermiculites
		Diocahedral vermiculites	Diocahedral vermiculites
	Mica	Trioctahedral micas	Phlogopite, biotite, lepidolite
		Diocahedral micas	Muscovite, paragonite
	Brittle mica	Trioctahedral brittle micas	Clintonite, anandite
		Diocahedral brittle micas	Margarite
Chlorite	Trioctahedral chlorites	Clinochlore, chamosite, nimate	
	Diocahedral chlorites	Donbassite	
	Di,triocahedral chlorites	Cookeite, sudoite	
2:1 inverted ribbons	Sepiolite - palygorskite	Sepiolites	Sepiolite, loughlinitite
		Palygorskites	Palygorskites

2. Methods

2.1 Microscope

Binocular scope with external light source. The model of the microscope used to look at hand sized samples is Leica MZ12 which has 10x standard magnification which up to additional 10x magnification can be added. This microscope was equipped with a manageable lamp on the right and left side.

2.2 Thin sections

Five thin sections were prepared by sawing areas of interest into approximately 2 x 1.5 x 1 cm pieces and sent to laboratory for production by Joakim Mansfeld. The aim was to make two thin sections to observe the contact with each rock (fine-grained mafic and granitic gneiss) on each side of it. But as the core sample split into two pieces along the contact then three thin sections were made instead, where one was fine-grained mafic rock with contact and two were granitic gneiss with contact. A fourth thin section was made of unaltered fine-grained mafic rock with black vein while the fifth was fine-grained mafic rock with two different hues of mafic.

The thickness of the sample in the thin section is 30 μm thick as the standard for interference colour observation is the chart by Michel-Lévy. The petrographic microscope model used for thin section observation is Leica DFC320 with three settings that is reflective, XPL (cross polarised light) and PPL (plane polarised light). Minerals are identified by colour, pleochroism, relief, crystal form, crystal texture, interference colours and cleavage.

2.3 XRD (X-ray Powder Diffraction)

XRD is a rapid (~20 min) analytical technique used for phase identification of a crystalline material based on the unit cell dimensions and atomic spacing. The X-ray is generated by a cathode ray tube which is filtered to produce monochromatic radiation that is directed toward the sample. The rays are diffracted and produce a constructive interference when the conditions satisfy Bragg's Law ($n\lambda=2d \sin \theta$). This law relates the wavelength of the radiation to the diffraction angle and lattice spacing in the sample. After the diffracted x-ray is detected it is processed and counted.

As crystals can favour certain orientation in the sample, analysing the sample from multiple angles is required in order to acquire correct unity of the sample. X-ray diffractometers work by rotating the sample in the path of the collimated X-ray beam at angle θ while the detector rotates at an angle of 2θ . For typical powder patterns, the data is collected at 2θ from an angle from $5 - 70^\circ$, the diagrams show count on Y-axis and angle on X-axis. The setting used for this study were $5 - 60^\circ$, X-ray at 45kV and rayons at 40mA. This method requires a small piece from the sample rock to be ground into powder. The XRD provides qualitative rather than quantitative data. Quantitative data can be assessed with the assistance of the software "Rietveld Refinement". Nine analyses were processed, only one set of quantitative data was provided for the fine-grained mafic rock due to economic constraints.

2.4 XRF (X-ray Fluorescence)

This method is used to get bulk composition of sample rock by analysing the behaviour of major and trace element atoms when interacting with radiation. High-energy such as short wavelength radiation (X-ray) ionise material. When energy becomes high enough it can dislodge the tightly held inner electron. In order for the atom to remain stable an outer electron replaces the missing inner electron, releasing additional energy (outer electron contains more energy than inner electron). This emitted radiation has

lower energy than the primary incident X-rays and is called fluorescent radiation. Each element has a unique fluorescent radiation energy.

A total of 43 measurements was taken with the XRF focusing on the black vein, fine-grained mafic rock, contact and granitic gneiss respectively.

3. Result

3.1 Microscope

Black vein

A black line (vein) in grey rock with directed orientation of the surrounding grey minerals, see **fig 8**.

Figure 8: The figure (left) shows shearing along the black vein in x100 magnification, see red arrows for shear sense and blue for suggested direction (sinistral shear).



Contact

The figures below (**fig 9, 10 and 11**) show different minerals that can be observed in the contact.

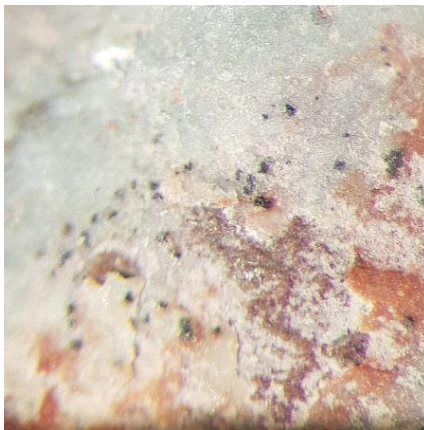


Figure 9 (above): shows calcite (white), chalcopyrite (reddish gold), hematite (black) and red unknown crystals.

Figure 10 (below): shows the brownish altered fine-grained grey rock and white calcite with black mineral that is hematite.

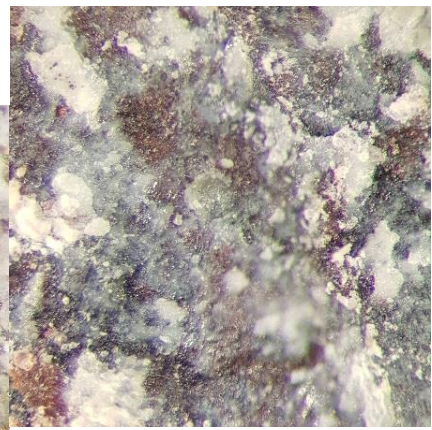
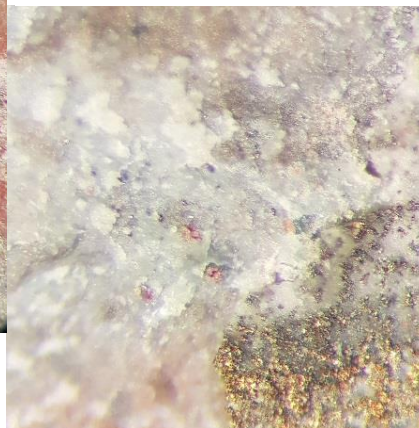


Figure 11 (above): shows calcite, brownish altered fine-grained grey rock and a yellowish green mineral that could be brucite (see section XRD).

3.2 Thin section

Black vein

The black vein can be observed in the figures below. **Fig 12** shows a plagioclase crystal that been sheared, the direction of the shear is hard to observe as there is some random orientated crystals in the matrix. Opaque minerals can be observed in the vein of **fig 13**. There are two types of veins in the fine-grained mafic rock: Chlorite and chlorite plus calcite can be observed in the thicker veins such as in **fig 13**.

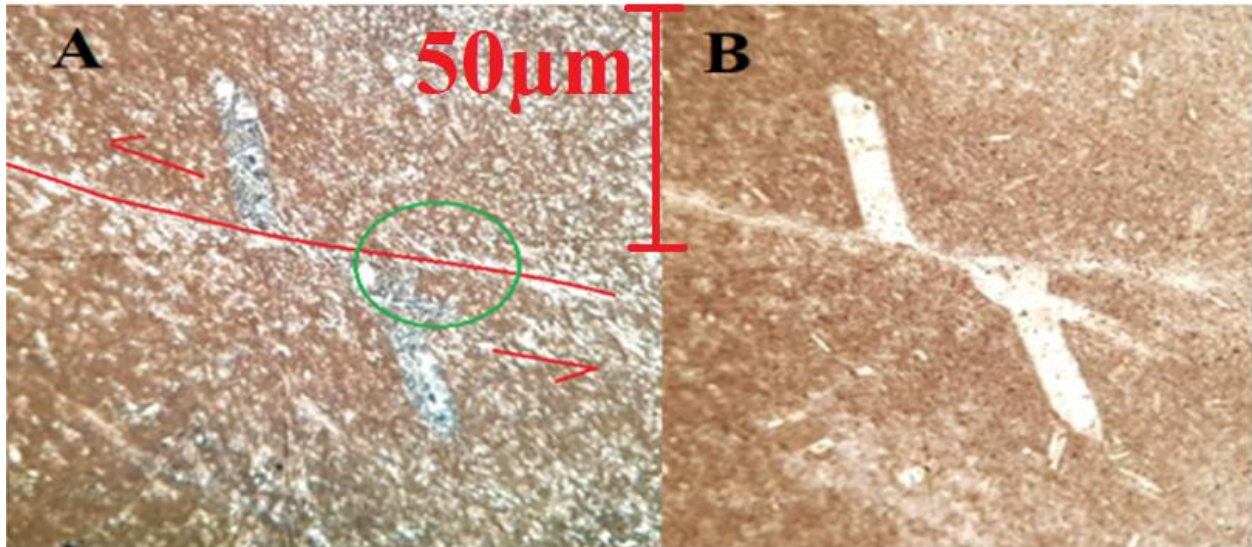


Figure 12: This figure (below) shows shearing that broken the large crystal along the shear plane in thin section. Left (A) shows in XPL and right (B) in PPL. Suggested directions are marked with red arrow (sinistral), green circle shows shear sense along the vein.

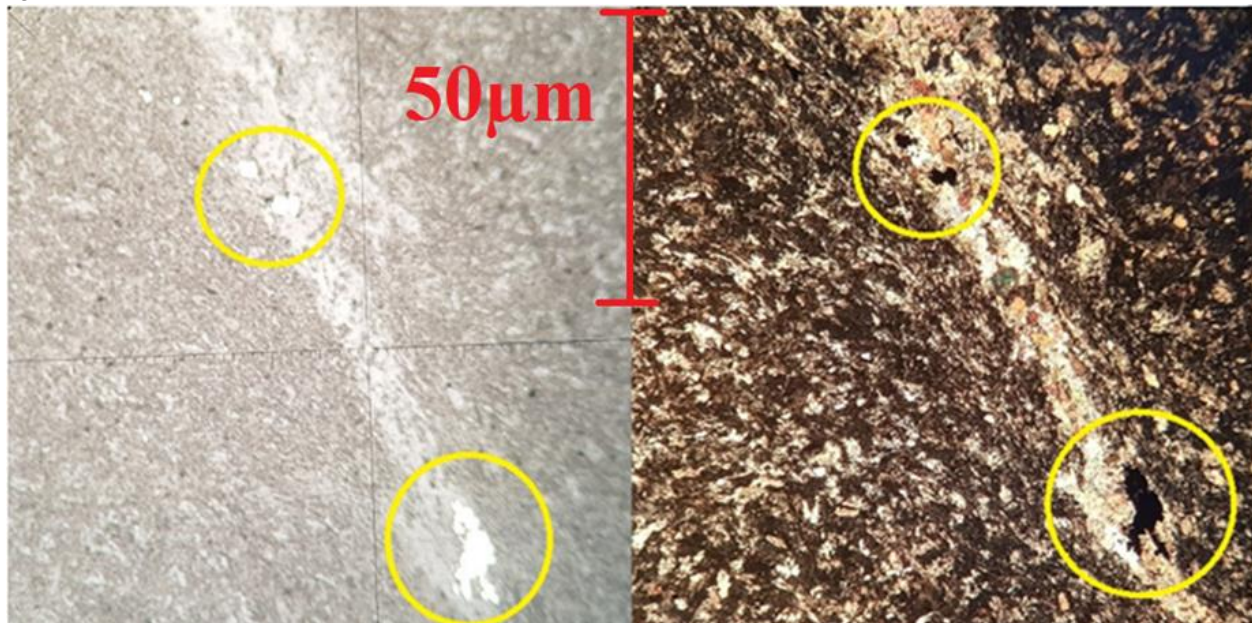


Figure 13: Opaque minerals in the vein made of chlorite and calcite can be observed in PPL and XPL. These minerals are identified as sulphide mineral chalcopyrite by using reflective light on the microscope. In this microscopic setting they appear metallic greenish yellow.

Fine-grained mafic rock

Less altered plagioclase crystals can be observed as they are widely spread across in this rock (**fig 14**). Chlorite, sericite, muscovite can be observed in the fine-grained mafic rock matrix. Relict plagioclase phenocrysts replaced with sericite and muscovite can be observed in **fig 15**. Chlorite is very abundant as well but is hard to observe in magnification less than 63x (**fig 16**). The fine-grained mafic rock is more or less completely altered into clay sized minerals where the only sign of the unaltered rock is plagioclase crystal relics.



Figure 14: Multiple plagioclase phenocryst can be observed.

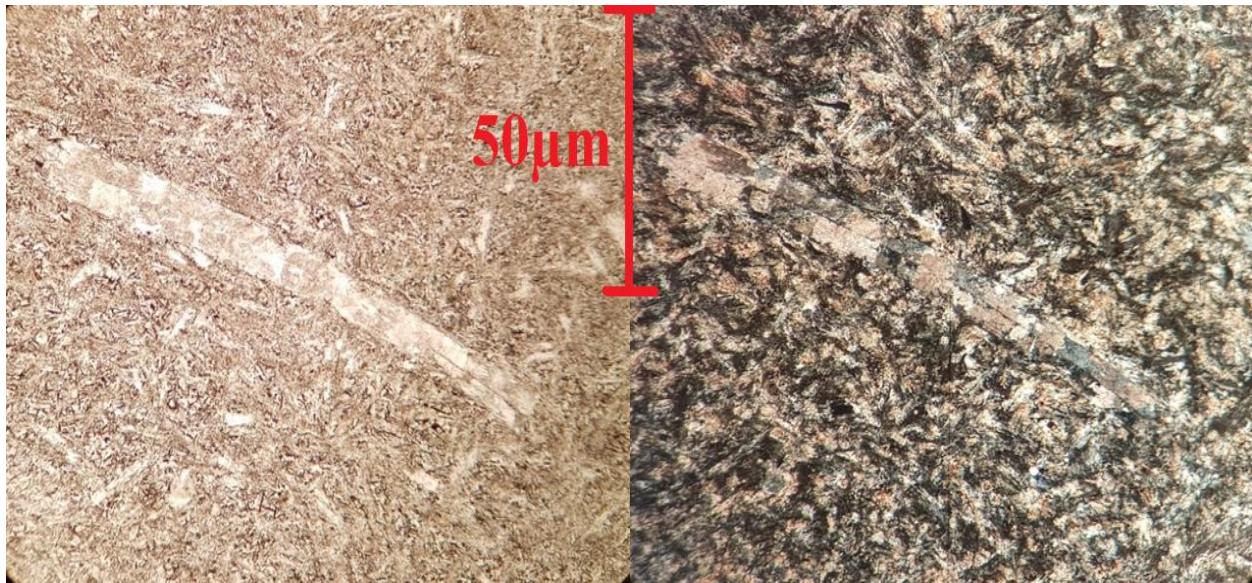


Figure 15: The left figure shows a plagioclase relic in PPL. The right figure shows in XPL that the crystal has been replaced by other minerals as it has the same characteristics as the matrix that consist of very fine crystals of muscovite, quartz, albite, sericite and chlorite.

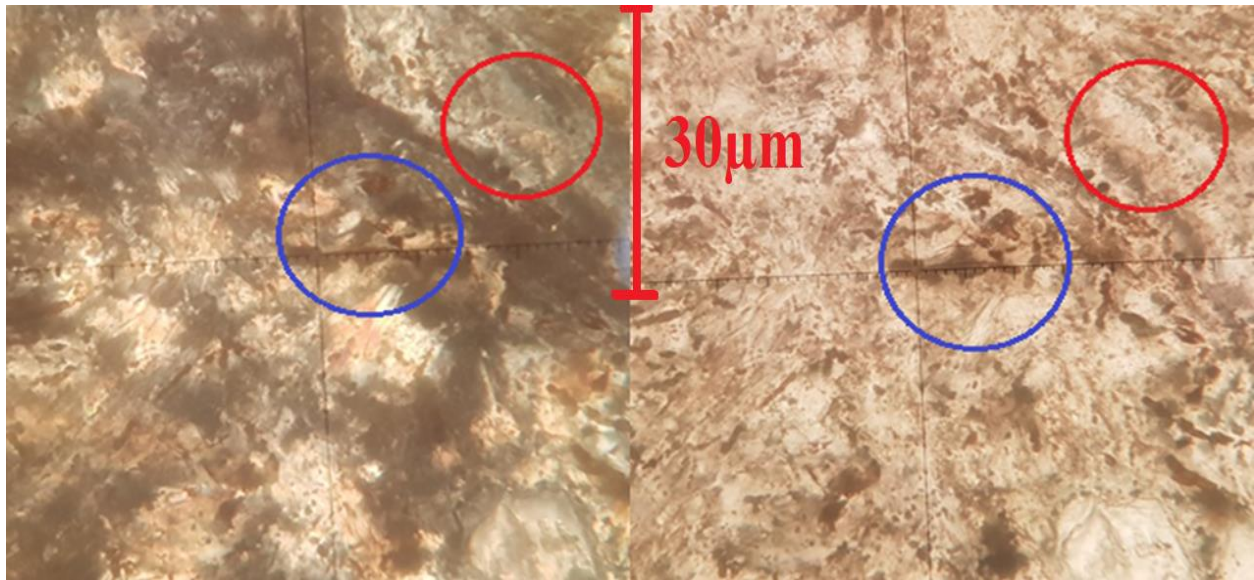


Figure 16: This figure is 63x magnified. Chlorite (red circle), sericite (matrix) and brown crystals (blue circle) can be observed. The chlorite is greenish (XPL/PPL) and has medium relief (PPL). These crystals have slightly higher relief and are easily seen in both XPL and PPL. Muscovite / sericite surrounds these minerals as a light brownish orange mineral in XPL and colourless in PPL. The brown is most likely an unidentified mineral as they have prismatic crystal habit rather than iron hydroxide.

Contact

The contact alters both rocks differently, diffusion can be observed in the fine-grained mafic rock (A-E) while it appears to penetrate between grains in the granitic gneiss (1-6). The general appearance in the fine-grained mafic rock is more alteration toward the contact that be separated into three layers (B-D) in **fig 17**. The layer between the fine-grained mafic rocks contact made of (A, medium-grained quartz) and the calcite vein (1) is missing due to breakage during thin-section preparation. Some opaque mineral grains and tightly amassed iron hydroxides can be observed in layer B, thin quartz or calcite veins penetrates this section but not into layer C. In layer C the iron hydroxides are not as tightly amassed as in layer B, there is no opaque mineral in this section. The iron hydroxide is widely spread across layer D, they are cannot be distinguished from the matrix except by the light brown colour.

Section 2 (fine-grained quartz) is the middle part of the contact with either calcite vein (1 and 4) or medium-grained quartz (A and 3) along the sides. Layer 5 consists of calcite with enrichment in iron hydroxide. The calcite vein (4) penetrates layer 2 and 3 as well the granitic gneiss (layer 6). **Fig 18** shows formation of iron sulphides (pyrite and chalcopyrite) and iron hydroxides in the granitic gneiss as well along the calcite vein. Different microscopic settings are used to distinguish the sulphides and hydroxides: reflective (left), XPL (middle) and PPL (right).

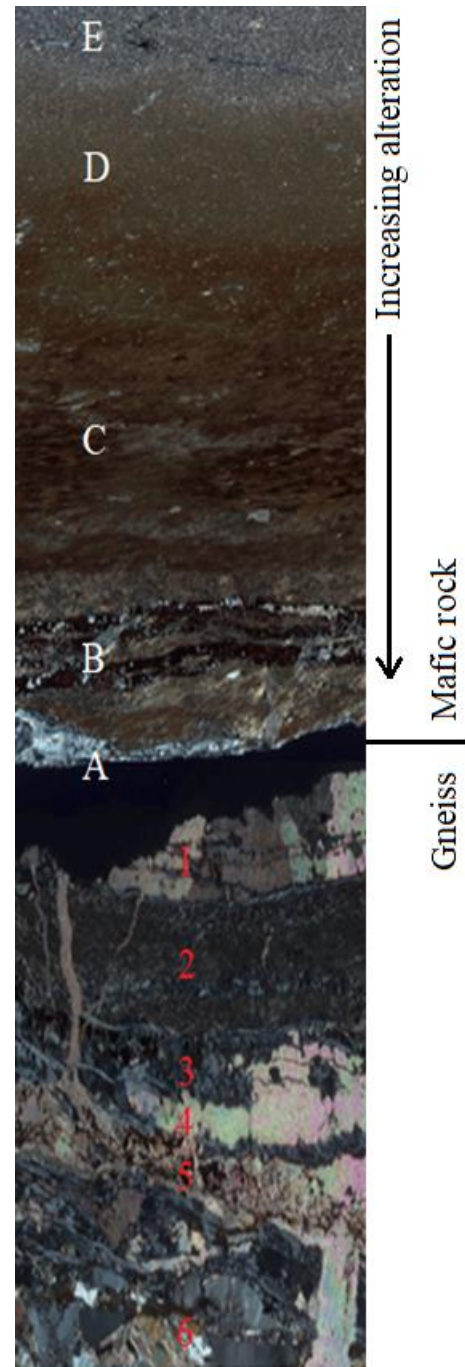


Figure 17: (right) shows an overview of the contact and area of alteration. The fine-grained grey rock (top) shows stronger alteration towards the contact (section A) where section E is unaltered. Different types of veins such as calcite (1, 4 and 5) and quartz (2 and 3) can be observed in the bottom section (granitic gneiss).

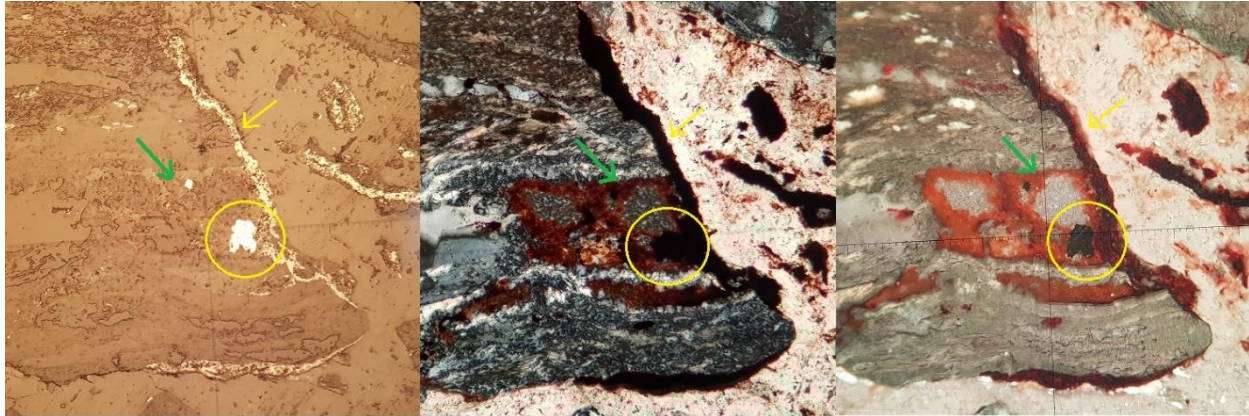


Figure 18: Three different opaque minerals. The yellow circle shows a mineral with the strongest reflection is a pyrite grain, the green arrow shows an opaque mineral with medium reflection being chalcopyrite surrounded by reddish iron hydroxide. The yellow arrow shows an opaque mineral with low reflectance being chalcopyrite combined with iron hydroxides. These minerals are likely formed when mobile metals react with sulphur transported by the contact fluid.

Granitic gneiss

The granitic gneiss is dominated by quartz, albite, biotite and muscovite, less abundant minerals such as chlorite, pyrite, chalcopyrite, hematite and iron hydroxide can be identified as well. **Fig 19** shows minerals in different microscopic setting; reflective (left), XPL (middle) and PPL (right). In **fig 20** co-existence of muscovite and biotite can be observed as well as quartz and chlorite.

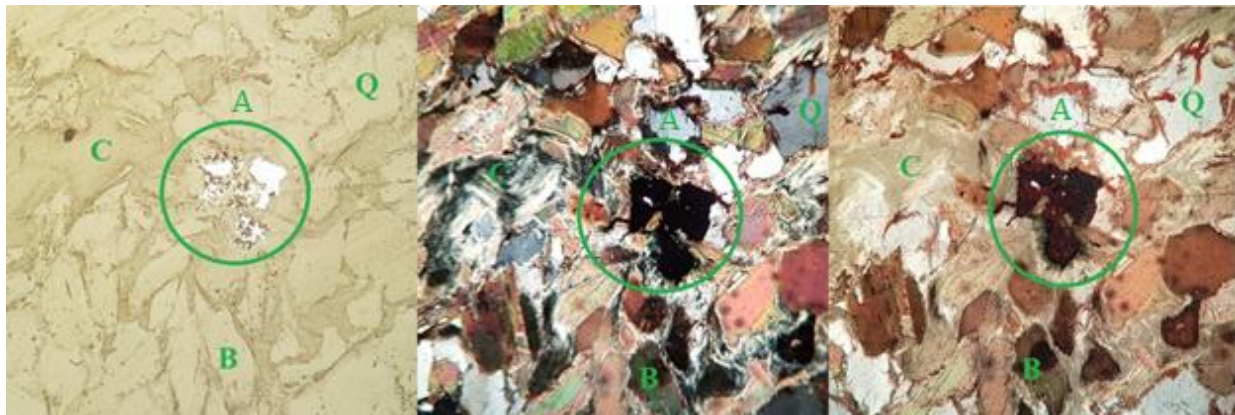


Figure 19: Quartz (Q), albite (A), biotite (B) and chlorite (C). The green circle shows an opaque mineral grain with red rim in PPL, this mineral is chalcopyrite with iron oxidised rim.

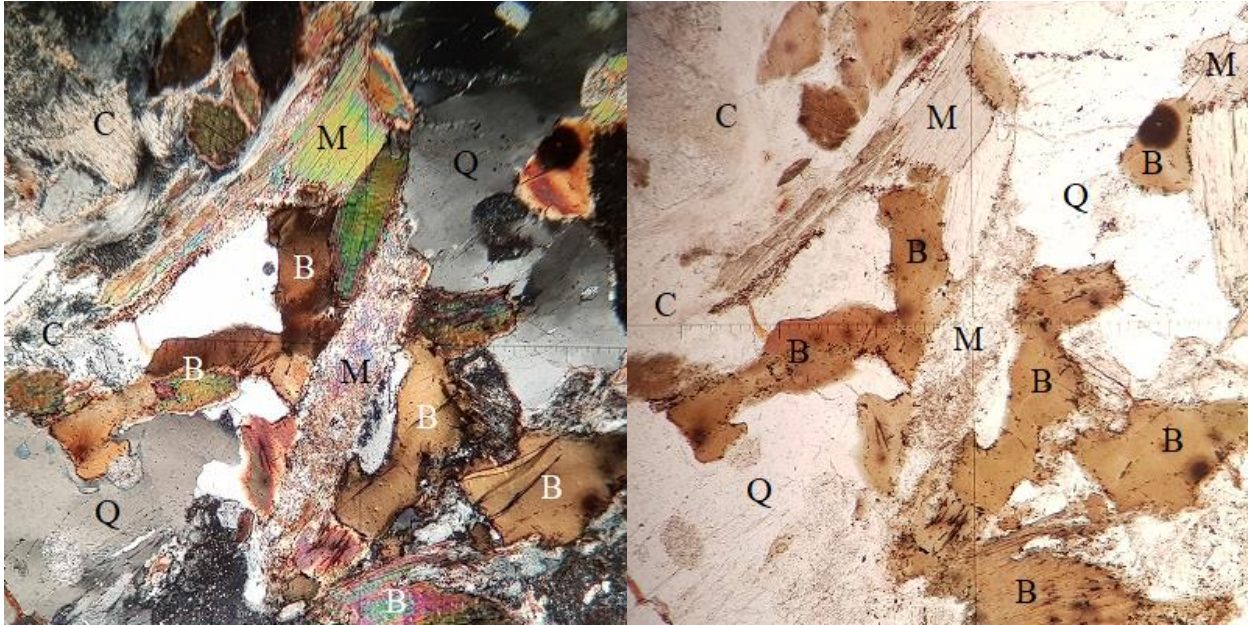


Figure 20: Muscovite (M), biotite (B), quartz (Q) and chlorite (C). Biotite can be distinguished from muscovite by the brown colour in PPL (right).

3.3 XRD Black vein

Mineral assemblage by XRD: Albite, calcite, chlorite and quartz

Fine-grained mafic rock

Mineral composition and quantitative calculation were obtained by XRD with assistance of a Rietveld Refinement software was determined to be:

Muscovite (36,1%), quartz (24,6), albite (20,8%), sericite (10,8%), iron-rich chlorite var. chamosite (7,3%) and montmorillonite $(\text{Na,Ca})_{0,33}(\text{Al,Mg})_2(\text{Si}_4\text{O}_{10})(\text{OH})\cdot n\text{H}_2\text{O}$ (0,5%); see **fig 21** (right) for an overview.

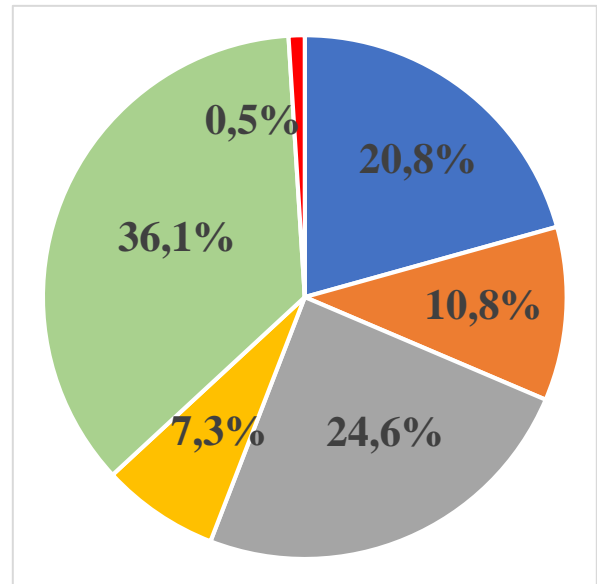


Figure 21: circle diagram of the composition of the fine-grained grey rock.

Contact

Five different sections of the contact were analysed.
See **fig 22**.

The XRD suggest a mineral composition for the sections:

(A) calcite, hematite, magnetite and brucite $\text{Mg}(\text{OH})_2$.

(B) quartz, albite, siderophyllite $\text{KFe}^{2+}_2\text{Al}(\text{Al}_2\text{Si}_2)\text{O}_{10}(\text{F},\text{OH})$,
chlorite, iron hydroxides and hetaerolite $\text{ZnMn}^{3+}_2\text{O}_4$.

(C) quartz, albite, chlorite and iron hydroxides.

(D) calcite and hematite. (E) calcite and quartz.

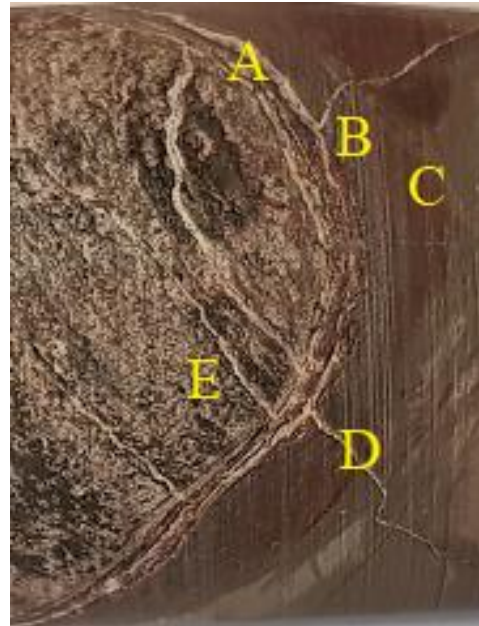


Figure 22 (above); white vein (A) between unknown rock and granitic gneiss. Fine-grained grey rock direct contact with the vein (B) and fine-grained grey rock further away from vein than B but still show some alteration by looking red (C). White vein intruding fine-grained grey rock (D) and white vein intruding granitic gneiss (E).

Granitic gneiss

According XRD there is quartz, albite, biotite, sericite, calcite and muscovite in the granitic gneiss.

3.4 XRF

All samples except the black vein show 0 % Mg because the XRF has difficulties distinguishing values of Mg less than 3% (Mansfeld, 2019). Therefore, an assumption of 1,5% Mg is taken. See **table 3** for overview of element composition of the rocks: fine-grained mafic rock, black vein, contact and granitic gneiss.

Table 3: mean major and trace elements content of fine-grained mafic rock, black vein, contact and granitic gneiss.

wt%	Fine-grained mafic rock	Black vein	Contact	Granitic gneiss
SiO ₂	65,20 ± 1,00	44,01 ± 1,29	22,23 ± 3,74	65,12 ± 6,70
TiO ₂	2,03 ± 0,21	0,22 ± 0,03	15,80 ± 10,73	0,61 ± 0,14
Al ₂ O ₃	13,92 ± 0,35	15,78 ± 0,35	9,21 ± 1,95	16,96 ± 3,15
Fe ₂ O ₃	9,27 ± 0,93	25,27 ± 0,82	5,53 ± 2,20	10,75 ± 3,05
MnO	0,16 ± 0,02	0,19 ± 0,02	1,37 ± 0,70	0,12 ± 0,03
MgO	1,50 ±	9,87 ± 1,39	1,50 ±	1,50 ±
CaO	4,77 ± 1,04	1,63 ± 0,98	43,96 ± 15,78	0,48 ± 0,41
K ₂ O	4,07 ± 0,40	2,54 ± 0,48	1,41 ± 0,37	5,40 ± 1,00
P ₂ O ₅	0,02 ± 0,05	0,00 ±	0,10 ± 0,20	0,11 ± 0,11
SO ₂	0,00 ±	0,00 ±	0,03 ± 0,06	0,00 ±
ppm				
V ₂ O ₃	83,4 ± 18,2	40,3 ± 8,0	73,8 ± 93,6	73,7 ± 17,9
Cr ₂ O ₃	51,1 ± 5,6	4,9 ± 8,5	10,4 ± 20,8	26,6 ± 7,3
CoO	57,8 ± 10,9	107,7 ± 16,6	28,5 ± 32,9	67,4 ± 12,3
NiO	21,5 ± 3,8	31,8 ± 4,8	11,1 ± 8,9	14,2 ± 4,9
CuO	54,3 ± 25,7	13,6 ± 4,7	6,0 ± 7,6	4,7 ± 2,3
ZnO	8,4 ± 1,0	53,5 ± 5,8	0,0 ±	14,0 ± 4,8
ZrO ₂	25,2 ± 1,0	14,5 ± 2,0	6,3 ± 12,6	21,9 ± 6,6
Ag ₂ O	32,1 ± 1,8	10,9 ± 18,8	22,6 ± 26,1	29,9 ± 2,4
CdO	41,8 ± 2,6	39,8 ± 2,0	43,2 ± 28,9	37,5 ± 3,4
SnO ₂	50,4 ± 3,4	47,3 ± 1,8	46,2 ± 31,3	45,5 ± 4,4
PbO	0,0 ±	2,4 ± 1,3	0,0 ±	1,2 ± 0,8
Bi ₂ O ₃	1,8 ± 1,7	4,4 ± 0,5	0,0 ±	5,1 ± 1,5
n	9	5	4	7

4. Discussion

This discussion focus on the evolution of the fine-grained mafic rock, the formation sequence of fine-grained mafic rock, black vein, contact and granitic gneiss. The granitic gneiss will not be discussed as the results does not deviate from known composition. Metamorphic grade could have been investigated but is outside the scope of this study.

4.1 Fine-grained mafic rock

No metamorphic texture such as cleavage, foliation or folding can be seen with the aid of microscope. Although shearing can be observed which results in the black veins as chlorite is enriched in it. There is no crossing of the black vein and the calcite vein, it is therefore not possible to guess which of them appeared first respectively last. A few larger crystals observed in this is rock suggest the grain size varied in the rock suggests an original porphyritic texture. During alteration the smaller crystals are more easily affected than the larger crystals. Many minerals in the rock are typically alteration products such as muscovite, sericite and chlorite.

Pure albite is not common as igneous rock, as Bowen's reaction series would transform it into alkali feldspar or clay and thus is probably an alteration product of sericitisation and/or albitisation. A dominating amount of muscovite (36.1%) and sericite (10.8%) suggest a high K content feldspar after Ca-plagioclase. Muscovite and sericite are the product of sericitisation of K-feldspar. Quartz (24,6%) and albite (20,8%) is like to be by-product of this sericitisation. Na content changes from the protolith to the altered rock cannot be observed as assistance of other methods would have been required. This makes the origin of Na more difficult to determine. Still, the presence of albite it is most likely due to Na assimilation after sericitisation of K-feldspar.

The chlorite could have been produced by alteration of mafic minerals or product of Fe/Mg injection to alter muscovite. The K loss from muscovite alteration is likely to be absorbed by albite sericitisation to produce more muscovite. The absence of sulphides and carbonates except in the veins suggest a fluid poor or depleted in sulphur or carbon as pyrite and calcite are easily produced in low temperature.

There is roughly 5% Ca in the fine-grained mafic rock, this could either be in montmorillonite, calcite undetected by the XRD or presence in the Na-plagioclase. As K content governs the reaction of Ca-plagioclase to K-feldspar, insufficient K could result in some remaining Ca-plagioclase. The black

vein that is produced from shearing that also produces small amounts of calcite and sulphides, highlighting that the amounts of S and C are small.

Suggested reaction pathways are shown in **fig 23**. The Ca-plagioclase (potential Na content) is altered into K-feldspar as the K replaces Ca. Ca could either become calcite in the presence of CO₂ or dissolved in the fluid, in this case Ca is probably dissolved as calcite is absent due to open system. The K content is then dissolved into muscovite due to sericitisation which produces Na-plagioclase (potential K content) and quartz.

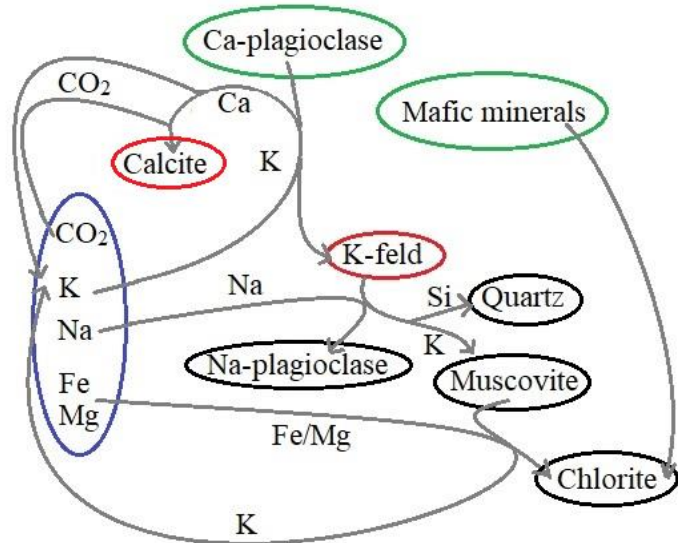


Figure 23: Reaction pathway, minerals of protolith (green), absent minerals (red), fluid (blue) and minerals in mafic rock (black).

By comparing immobile elements with previous studies of samples from the area, a suitable suggestion can be made by minimal changes in immobile elements. In this case, Al and Ti content of a gabbro matches the Al and Ti content in the fine-grained mafic rock, see **fig 24**.

Enrichment of Fe is visible along the contact, indicated by the reddish-brown colour and higher content of chlorite. Chlorite can be produced through two pathways: either through chloritisation of mafic minerals or of muscovite in presence of Fe and Mg. Identifying which of these reactions has occurred in our case could give important clues about the content of Fe and Mg present in fluids during the alteration

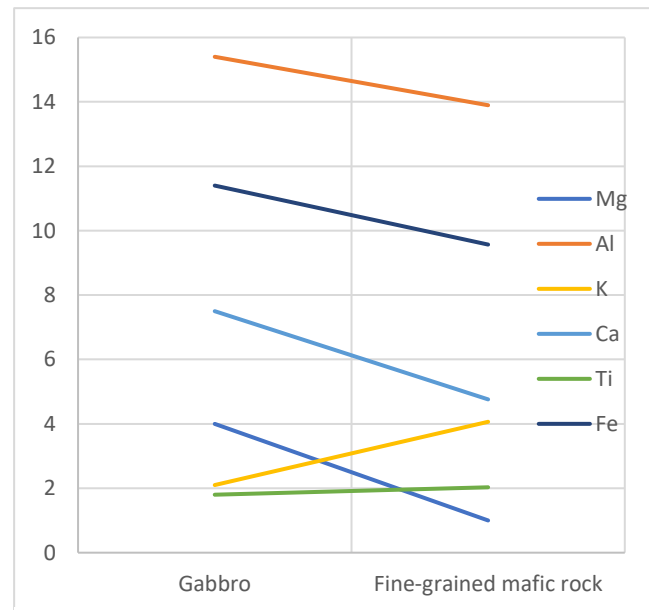


Figure 24: Comparison of immobile elements content (Al and Ti) between the suggested protolith (a gabbro, on the left) and the fine-grained mafic rock (right). Evolution of mobile elements can be observed where K is enriched while Fe, Ca and Mg is depleted.

processes and about the protolith. If the chlorite was formed through chloritisation of mafic minerals, it shows that the mafic minerals of the protolith were iron rich. If it instead was formed through alteration of muscovite, it would show that the fluids present during the alterations were rich in Fe and Mg. In this

case, decreasing Fe and Mg suggest an domating mafic mineral alteration process with Fe and Mg loss into fluids as well rather than influx on Fe and Mg. The difference of these elements is rather small which could be an error of different gabbro composition compared the core sample area. In order to get a more accurate interpretation, data from nearby gabbro or dolerite would be needed.

4.2 Contact

Knowledge of the contact is important as it provides information of the formation sequence of surrounding rocks. The fine-grained mafic rock is altered by showing signs of iron enrichment along the contact shows higher grade of alteration with increased enrichment of iron hydroxides. The granitic gneiss is affected by calcite intrusion and is enriched of iron hydroxides along the contact as well. The general profile of the contact is medium-grained quartz, calcite and fine-grained quartz towards the centre.

The suggested formation sequence of the core sample can be observed in **fig 25**. The granitic metamorphism is older than the dolerite intrusion as the dolerite is not metamorphosed. The dolerite along the contact is altered and the contact appears to intrude in between the granitic gneiss and dolerite.

**Granitic gneiss Dolerite Quartz vein Calcite vein
Shear**

Figure 25: Formation sequence of the core sample, old (left) towards young (right).

The calcite vein in the contact is younger than the quartz vein as it penetrates the wall of the quartz vein into the granitic gneiss. But such side-penetrating calcite veins into the fine-grained mafic rock cannot be observed. Although there are calcite veins observed in the fine-grained mafic rock, these could have another source. The chlorite shear veins cannot be observed crossing the calcite vein in the fine-grained mafic rock, therefore the sequence of them are uncertain.

5. Conclusions

The formation sequence of the rock is shown in detail in **fig 25**. This sequence is provided by interpretation of metamorphism (gneiss is affected while mafic rock is not) and intruding veins. The fine-grained mafic rock is a heavily altered dolerite with the composition observed in **fig 24**. The protolith interpretation is made by comparing the immobile elements Al and Ti.

6. Further studies

In order to obtain a more detailed understanding there are some aspects of this work that needs some further investigation.

- 1) Identify the unknown mineral in the dolerite. This can provide more information about the alterations processes.
- 2) EDS, chemical composition of the dolerite minerals for more specific mineral species of e.g. chlorite.
- 3) Find a more suitable protolith for more precise immobile element content evolution.
- 4) Whole rock analysis, Na analysis of the altered and the unaltered dolerite for a deeper understanding of the alteration processes.
- 5) Larger study area to understand the spread of the alteration level of the dolerite
- 6) Study physical properties such as strength and durability of dolerite with different alteration levels

7. References

Brindley, G. W., Brown, G., 1984, Crystal structures of clay minerals and their x-ray identification, Mineral Society

ISBN 0144-1485 / 0-903056-08-9

Carroll, D., 1970, Rock weathering, Springer US

ISBN 978-1-4684-1794-4

Winter, J. D., 2014, Principles of igneous and metamorphic petrology, 2nd E, Pearson

ISBN 10: 1-292-02153-5

Lagat, J., 2008, Hydrothermal alteration mineralogy in geothermal fields with case examples from Olkaria Domes geothermal field, Kenya

Lal, R., 2002, Encyclopedia of soil science, Marcel Dekker

ISBN 978-849350535

Lundqvist, J., Lundqvist, T., Lindström, M., Calner, M., Sivhed, U., 2011, Sveriges geologi från urtid till nutid, Studentlitteratur

ISBN 9789144058474

Mansfeld, J., 2019, Personal XRF experience

Mathieu, L., 2018, Quantifying hydrothermal alteration: A review of methods. Centre D'études sur les Ressources Minérales (CERM)

Nelson, S. A., 2018, Petrology: Types of metamorphism
(<https://www.tulane.edu/~sanelson/eens212/typesmetamorph.htm>)

SGU, Map series K439, 2013

Stephens, M. B., Ripa, M., Lundström, I., Persson, L., Bergman, T., Ahl, M., Wahlgren, C., Persson, P., Wickström, L., 2009, Synthesis of the bedrock geology in the Bergslagen region, Fennoscandian Shield, south-central Sweden, Geological Survey of Sweden

ISBN 978-91-7158-883-8

Wilson, M., 1995, A global tectonic approach, Chapman & Hall

IBSN 0-412-53310-3